HHS Public Access

Author manuscript

J Biomech. Author manuscript; available in PMC 2015 July 29.

Published in final edited form as:

J Biomech. 2013 May 31; 46(9): 1540–1547. doi:10.1016/j.jbiomech.2013.03.021.

Azidothymidine (AZT) leads to arterial stiffening and intima-media thickening in mice

Laura Hansen[a], **Ivana Parker**[b], **LaDeidra Monet Roberts**[a], **Roy L. Sutliff**[c], **Manu O. Platt**[a,d], and **Rudolph L. Gleason Jr.**[a,b,d,*]

[a]The Wallace H. Coulter Department of Biomedical Engineering, Georgia Institute of Technology, Atlanta, GA, USA

[b]The George W. Woodruff School of Mechanical Engineering, Georgia Institute of Technology, Atlanta, GA, USA

[c]Department of Medicine, Emory University, Atlanta VAMC, Atlanta, GA, USA

[d]The Petit Institute for Bioengineering and Bioscience, Georgia Institute of Technology, Atlanta, GA, USA

Abstract

HIV positive patients on highly active antiretroviral therapy (HAART) have shown elevated incidence of a number of non-AIDS defining co-morbidities, including cardiovascular disease. Given that HAART regimens contain a combination of at least three drugs, that disease management often requires adjustment of these regimens, and HIV, independent of HAART, also plays a role in development of co-morbidities, determining the role of specific HAART drugs and HIV infection itself from clinical data remains challenging. To characterize specific mediators and underlying mechanisms of disease, in vitro and in vivo animal models are required, in parallel with clinical data. Given its low cost azidothymidine (AZT) contributes to the backbone of a large proportion of HAART treated patients in the developing world where much of the global burden of HIV resides. The goal of this study was to test the hypothesis that AZT can lead to proatherogenic changes including the subclinical markers of arterial stiffening and intima-media thickening in mice. AZT (100 mg/kg) or vehicle was administered to wild-type FVB/N mice via oral gavage for 35 days. Cylindrical biaxial biomechanical tests on the common carotid arteries and suprarenal aortas exhibited arterial stiffening in AZT mice compared to controls. Multiphoton microscopy and histology demonstrated that AZT led to increased intima-media thickness. These data correlated with decreased elastin content and increased protease activity as measured by cathepsin zymography; no differences were observed in collagen content or organization, in vivo axial stretch, or opening angle. Thus, this study suggests the drug AZT has significant effects on the development of subclinical markers of atherosclerosis.

*Correspondence to: The Petit Institute for Bioengineering and Bioscience, Georgia Institute of Technology, 315 Ferst Drive, IBB 2305, Atlanta, GA 30332, USA. Tel.: +1 404 385 7218; fax: +1 404 385 1397. rudy.gleason@me.gatech.edu, rudolph.gleason@bme.gatech.edu (R.L. Gleason Jr.).

Conflict of interest

We have no conflict of interest to report.

Keywords

HIV; HAART; Atherosclerosis; Arterial remodeling; Non-AIDS defining illnesses

1. Introduction

The development and widespread use of highly active antiretroviral therapy (HAART) has drastically increased the life expectancy of HIV patients; however, HAART drugs have been implicated in the early on-set and increased risk of numerous co-morbidities, including cancers, central nervous system disorders, pulmonary disease, renal disease, hepatic disease, diabetes, and cardiovascular disease. Cardiovascular complications include increased incidence of myocardial infarction (Friis-Møller et al., 2003; Mary-Krause et al., 2003; Holmberg et al., 2002) and atherosclerotic lesions (Maggi et al., 2004; Spieker et al., 2005) and elevated preclinical markers of atherosclerosis (e.g., increased carotid intima-media thickness (c-IMT) (van Vonderen et al., 2009; Hsue et al., 2004; Ross et al., 2008), arterial stiffening (van Vonderen et al., 2009; Bonnet et al., 2004; Sevastianova et al., 2005), and impaired flow mediated dilation (FMD) (Bonnet et al., 2004; Calmy et al., 2009; Shankar et al., 2005). Antiretrovirals are typically prescribed in cocktails of three drugs; thus, the roles of specific HAART drugs in the development of atherosclerosis are difficult to determine from clinical data (Lundgren et al., 2008; Worm et al., 2010); viral infection may also play a significant role, further complicating the interpretation of clinical data (Oliviero et al., 2009; Hsue et al., 2009; El-Sadr et al., 2006). Thus, the use of laboratory models to quantify the role of specific HAART drugs and study the underlying mechanisms of disease progression is warranted.

Of the five classes of HAART drugs, nucleoside reverse transcriptase inhibitors (NRTIs), which include azidothymidine (AZT), and protease inhibitors (PIs) have been the most widely implicated drug classes in development of endothelial dysfunction Friis-Møller et al., 2003; Kline and Sutliff, 2008; Wang et al., 2007; Fisher et al., 2006). NRTIs make up the backbone of nearly all HAART regimens; thus, there is a pressing need to understand their role in the development and progression of atherosclerosis. Sutliff et al. previously found that administration of the drugs also increased endothelial cell death and increased vascular smooth cell replication, both of which disturb healthy vascular function. AZT administration in mice for 35 days led to endothelial dysfunction and increased superoxide levels (Sutliff et al., 2002). The purpose of this study was to quantify mechanical and geometric remodeling, including the development of arterial stiffening and intima-medial thickening, with AZT treatment in common carotid arteries and aorta in wild-type mice. We observed altered biomechanical remodeling, including arterial stiffening, intima-media thickening, decreased adventitia thickness, decreased elastin content, and differential cathepsin activity, with little difference in collagen content and fiber organization. Thus, AZT administration led to an increase in subclinical markers of atherosclerosis and these changes were associated with microstructural markers of vascular remodeling.

2. Methods

2.1. Animal treatment and artery isolation

Five week old male FVB/N mice (Jackson Labs) were administered 100 mg/kg azidothymidine (AZT) or water vehicle via oral gavage for 35 days. Male mice were used to minimize any variability due to the estrus cycle in females, and the age, strain, and dosage were chosen to match previous studies (Sutliff et al., 2002; Hansen et al., 2012). Non-invasive blood pressure monitoring was performed at 0, 17, and 35 days after initiation of treatment via a tail cuff system (Columbus Instruments). At the end of 35 days of treatment mice were euthanized with an intraperitoneal injection of sodium pentobarbital (100 mg/kg). Tissue was dissected and removed to expose both common carotid arteries and the aorta from the arch to the iliac bifurcation. Both common carotid arteries and the aorta were excised and cleaned free of perivascular tissue.

2.2. Biomechanical measurements: cylindrical biaxial testing, arterial stiffness, and opening angle

Cylindrical biaxial testing—Cylindrical biaxial biomechanical tests of the arteries were performed as previously described (Hansen et al., 2012). Excised common carotid arteries (3–5 mm long) and suprarenal aortas (4–5 mm long) were maintained in culture medium [Dulbecco's modified Eagles medium (Invitrogen, Inc.) containing 4.5 g/L glucose and sodium pyruvate and without L-glutamine and phenol red] in an incubator at 37 °C. 8–0 suture was used to mount the arteries on two glass cannulae on a custom biaxial mechanical testing device (Wan et al., 2010). Aortic branches within the suprarenal region were ligated using 10–0 silk sutures prior to cannulation. The vessel and cannulae were suspended in a bath on the device, which was filled with media containing sodium nitroprusside (SNP) to ensure that the arteries were fully dilated during the mechanical tests. This computer-controlled device is the capability of maintaining precise luminal pressure (± 1 mmHg) and axial length of the vessel (± 0.001 mm), while recording the outer diameter and axial force during the testing.

Vessels were preconditioned with three inflation cycles (0–160 mmHg) at a series of five axial stretches (λ = 1.5–1.9, λ is the loaded artery length/unloaded artery length). Fixed length pressure–diameter tests and fixed pressure force–length tests were performed under quasistatic loading conditions. During the pressure–diameter tests, vessels were inflated to 160 mmHg at a series of fixed axial stretches, λ = 1.3, 1.4, 1.5, 1.6, 1.7, 1.8, and 1.9, with three loading/unloading cycles for each axial stretch. During the force-length tests the vessels were held at constant pressures of 0, 40, 60, 80, 100, and 120 mmHg and stretched to an axial load of 1 g (for common carotid arteries) or 3 g (for the aorta) with three loading/unloading cycles at each pressure. Preliminary data (not shown) demonstrated that these loads were well above the in vivo loads and yielded repeatable mechanical loading curves over repeated cycles (i.e., these loads did not induce mechanical damage). In each of the testing protocols the third cycle was used for data analysis. The in vivo stretch was determined to be λ = 1.7 based upon the intersection of the force–length curves at this stretch (Wan and Gleason, 2010; Gleason et al., 2007; Dobrin, 1986; Takamizawa and Hayashi, 1987).

Arterial stiffness—The Peterson's modulus (E_p), a common measure of arterial stiffness, was calculated as the slope of the pressure–outer diameter curve ($\Delta P/\Delta D$) at a given pressure normalized to the outer diameter (D) at that pressure; namely, $E_p = (\Delta P/\Delta D)/D$.

Opening angles—Following testing or microscopy imaging (described below), ring sectors were cut from the arteries to obtain their stress free configuration following previous methods (Hansen et al., 2012). A 14% gelatin mixture was injected into the vessel and allowed to solidify, then the artery was cut into a series of segments and placed in phosphate buffered saline (PBS) (Wagenseil et al., 2005). A single radial cut was then made in each of these segments and the open sectors were allowed to equilibrate for 30 minutes. The vessel wall area A, inner arc length L_i, and outer arc length L_o were measure and the opening angle was then be calculated as $\theta = (L_o - L_i)/2H$ (Chuong and Fung, 1986).

2.3. Intima-media thickness measurements

The vessel wall thickness was quantified by two methods (confocal microscopy and histology), following previously described methods (Hansen et al., 2012).

Confocal microscopy—The testing device fits on a LSM 510 META inverted confocal microscope (Zeiss) to visualize the microstructure across the entire wall of live, unfixed mouse arteries (Wan et al., 2010). The vessel, maintained in PBS, was excited with a 800 nm two-photon laser, collagen was visualized by detecting its second harmonic generation around 400 nm, and elastin emissions were detected by setting the META filter to a 480–560 nm bandpass configuration (Zoumi et al., 2004). Z-stacks were collected at a variety of loading conditions including physiologic pressure and stretch. Orthogonal views of these z-stacks were then used to calculate the thickness of the adventitial layer (collagen images) and intima-media layer (elastin images) of the arteries.

Histology—Vessels were fixed in their unloaded state in 10% buffered formalin, immersed in 30% sucrose overnight, embedded in optimal cutting temperature medium, and frozen. The arteries were cut into 7 μm thick slices, mounted on slides, and stained with hematoxylin and eosin. The images were analyzed using ImageJ (NIH) to quantify the thickness of the arteries.

2.4. Collagen organization

Collagen fiber analysis—The multiphoton microscopy images were also used to quantify the angular distribution of fibers within the arterial wall. The angles of fibers in each slice of the z-stack were quantified using a fast Fourier series algorithm program in a MATLAB script as established previously (Ng et al., 2005; Timmins et al., 2010; Wan et al., 2012). The initial processing included low-pass filtering, converting to binary, and windowing with a 2D Tukey window. A fast Fourier transform of the preprocessed image generated a power spectrum. A histogram of the frequency of intensities between −90 and 90 degree with 4 degree bins was created from the spectrum. This process was repeated for each slice within the z-stack to generate a distribution of fibers across the wall for each vessel. The thickness and relative wall location were normalized and the corresponding distributions in each vessel were averaged to create a surface that represented the fiber angle

distributions through the wall, a mid-wall fiber distribution, and weighted mean fiber angle for comparison.

2.5. Collagen and elastin content

The Fastin assay (Biocolor) and Sirius red assay were used to quantify the elastin and collagen content of the dried arteries, following manufacturer instruction and as previously described (Hansen et al., 2012). Pairs of carotid arteries from a single mouse or a single suprarenal aorta were dried in a vacuum oven at 37 °C for 2 days. The dry weight of the vessels was recorded for normalizing protein content. The elastin content of the arteries was quantified using the Fastin Elastin Assay (Biocolor) and collagen via a Sirus red assay; see Hansen et al. (2012).

2.6. Cathepsin expression and activity measurements

Gelatin zymography was used to quantify the activity of cathepsins in the arterial walls. Excised suprarenal aortas or two pairs of carotids (4 arteries) were placed in 50 ul of lysis buffer (20 nM Tris–HCl [pH 7.5], 5 mM ethyleneglycoltetraacetic acid [EGTA], 150 mM NaCl, 20 mM β-glycerol phosphate, 10 mM NaF, 1 mM sodium orthovanadate, 1% Triton X-100, and 0.1% Tween 20) with 0.1 mM leupeptin freshly added to stabilize enzymes during electrophoresis, homogenized using disposable sample grinders (GE Healthcare), and protein concentrations were obtained by the bisinchoninic acid (BCA) assay (Pierce). Cathepsin zymography was performed as described previously (Hansen et al., 2012; Li et al., 2010; Wilder et al., 2011).

2.7. Statistical analysis

All data presented is mean plus or minus standard error mean (± SEM) (circular means and standard deviations were calculated for the weighted mean fiber angle analysis (Wan and Gleason, 2012). Means between groups were compared using unpaired student t tests with significance at $p < 0.05$. All statistics were performed in either Excel (Microsoft) or GraphPad Prism (GraphPad software).

3. Results

3.1. AZT treatment does not alter Blood pressure

No differences in the systolic blood pressure were observed between the AZT-treated and water-control mice at 0, 17, or 35 days of treatment (Fig. 1). Note that, as expected, blood pressure did increase during the experimental time course, due to maturation of the mice from 5 to 10 weeks.

3.2. AZT-treatment leads to arterial stiffening

Cylindrical biaxial tests revealed that 5 weeks of AZT treatment led to reduction in vessel caliber and increased arterial stiffness (Fig. 2). AZT treatment caused a downward shift in the diameter-pressure curve at the in vivo stretch ($\lambda = 1.7$); differences were significant at pressures of 10–60 mmHg for carotid arteries ($n = 6$) and 50–70 mmHg ($n = 8$) for aortas. The Peterson's modulus (E_p), a common measure of arterial stiffness, increased with AZT-treatment in the aorta; differences were significant at pressures between 10 and 50 mmHg.

Axial force, monitored during fixed length pressure–diameter tests, was lower with AZT treatment (Fig. 3); differences were significant at pressure between 10 and 80 mmHg in aorta ($n = 8$) at the in vivo stretch. No differences in axial force were observed in carotid arteries during the pressure–diameter tests or in the axial force-length curves in both the carotids and aortas. Additionally, no significant changes were observed in opening angle with AZT-treatment in carotids arteries or aorta (not shown).

3.3. AZT treatment leads to intima-media thickening

Stacks of multiphoton confocal images collected across the entire wall of arteries in a loaded configuration ($P = 100$ mmHg and axial stretch $\lambda = 1.7$) showed a significant increase in the intima-media thickness in the aorta (Fig. 4); no difference was observed in carotid arteries via this technique. Advential thickness decreased in both aorta and carotid arteries. Histological sections showed increases in intima-media thickness for both aorta and carotid arteries. Note that the nominal values for thickness from the microscopy versus histological techniques were different because the multiphoton microscopy measurements were taken in live vessels under physiological loading, while the histology measurements were taken from vessels fixed under no mechanical loading.

3.4. AZT treatment lowers elastin content, but does not alter collagen content and organization

Elastin content was decreased with AZT-treatment; significant differences were observed in the carotids (Fig. 6, $n = 6$). No differences in collagen content were observed with AZT treatment (not shown, $n = 6$). Stacks of multiphoton microscopy images were also used to quantify the organization of collagen fibers under physiological loading. No differences in the mean fiber angle were observed in aorta or carotid arteries with AZT (Fig. 5, $n = 6$).

3.5. AZT treatment differentially regulates cathepsin activity in carotids vs. aortas

Cathepsins are a family of proteases with potent elastolytic and collagenase activity. Mouse cathepsin L and cathepsin S, in particular, are powerful elastases. Densitometric analysis of the zymography gels showed changes in expression and activity between the AZT treated mice and the control mice. Specifically, carotid arteries from the AZT mice had over a 5-fold increase in cathepsin L activity compared to control mice (Fig. 7). Cathepsin L activity decreased with AZT treatment in aorta.

4. Discussion

van Vonderen et al. found a significant decrease in femoral artery distensibility and compliance between ART-naïve and ART-exposed patients indicating that antiretroviral treatment is likely a significant contributor to arterial stiffening in people living with HIV (van Vonderen et al., 2009). Charakida et al. (2009) also observed increased arterial stiffness (via pulse wave velocity measurements) in treated versus non-treated children living with HIV. Lorenz et al. (2008) found that HIV positive patients had increased cIMT as compared to control patients matched for traditional risk factors, and also that HAART treated patients had a 24.8% larger value for the carotid bifurcation intima-media thickness than the HAART naïve patients. Additionally, they report that NRTI use was associated with

increased cIMT, with the carotid bifurcation 28% or 48% higher in patients who had been on an NRTI for less than 1 year or more than 2 years respectively as compared to patients who were NRTI naive.

In vitro studies have shown that antiretroviral drugs (specifically AZT) have negative effects on vascular cells (Hebert et al., 2004), but the unique roles of anti-retroviral treatment and viral infection remains unclear. AZT was the first antiretroviral drug developed to treat HIV; although its use is declining in the developed world, given its low cost AZT contributes to the NRTI backbone of a large proportion of HAART treated patients in the developing world where much of the global burden of HIV resides. AZT administration in mice has previously been shown to lead to endothelial dysfunction and significantly increased superoxide levels in the vessel wall (Sutliff et al., 2002). The current study demonstrated that AZT administration leads to increased intima-media thickness and arterial stiffness in mice and that these observations will correlate with markers of microstructural remodeling; namely, decreases in elastin mass fraction and changes in cathepsin activity, which supports the findings of proatherogenic remodeling.

The use of a mouse model to study the effects of AZT allows one to not only isolate the influence of the drug from the influence of HIV infection or other lifestyle and risk factors present in clinical studies, but also allows one to study a number of parameters that are not clinically tractable. First, the use of a mouse allows one to investigate remodeling parameters in both the carotids and the aorta, which are both of clinical interest. Beyond analyzing the circumferential behavior, our rigorous mechanical testing protocols also investigated the axial behavior. While carotid arteries did not exhibit changes in axial behavior, the aortas from the AZT treated mice had lower axial forces at both in vivo and subphysiological stretches at pressures from 10 to 70 and 10 to 80 mmHg (Fig. 3). Differences in axial behavior are important since arteries respond to changes in axial loads (Gleason et al., 2007; Jackson et al., 2002; Humphrey et al., 2009), and there were differences in cathepsin activity (Fig. 7) between aortas and carotids which may play a role in axial behavior in aortas more than carotids. Another mechanical property we characterized that cannot be determined clinically is opening angle, a measure of residual stress. We did not see differences in the opening angles between the two groups indicating the vessels were able to maintain similar transmural distributions of stress, despite undergoing remodeling that resulted in changes in circumferential stiffness and intima-media thickness.

The vascular remodeling, which leads to the observed stiffening and thickening, is a complex process which involves both the synthesis and degradation of key ECM proteins (e.g., collagen and elastin) and cellular turnover and remodeling. In our studies we found a decrease in elastin content in the carotid arteries from the AZT treated mice (Fig. 6), which supports the observed arterial stiffening since elastin is the most compliant of the structurally significant constituents in an artery. Additionally, loss of functional elastin is associated with aging and a number of vascular diseases including aneurysm development and atherosclerosis (Fernandez-Moure et al., 2011; Lee and Oh, 2010). Mouse cathepsin L has been implicated in both biomechanically regulated elastase and collagenase activity (Platt et al., 2006a, 2006b), supporting the findings of this study. Zymography was used to

determine the activity of proteases within the wall, specifically that of cathepsins. Cathepsins are potent elastases and collagenases, thus their activity can lead to degradation of the ECM proteins within the wall. Increased cathepsin expression and activity has been associated with atherosclerosis (Sukhova et al., 2003; Shi et al., 2003; Platt et al., 2007). Cathepsin activity is upregulated in atherosclerotic lesions in humans (Shi et al., 1999; Sukhova et al., 1998; Liu et al., 2005); thus, the observed upregulation of cathepsin L (Fig. 7A) suggests a proatherogenic environment in the vascular wall of AZT treated mice (Platt et al., 2007). Additionally, we found a decrease in cathepsin L activity in the aortas. The reason for this downregulation is not clear from the literature but it is in agreement with our similar studies in an HIV transgenic mouse model and merits further investigation (Hansen et al., 2012). Another ECM parameter investigated was the organization of collagen fibers; though, no changes were observed (Fig. 5). While panel B (histogram of the mean intensities) may appear to show a difference between the groups, the weighted mean fiber angle calculated from these plots is not significantly different though the shape appears to vary. Note, the use of circular statistical methods to properly account for angles, makes the variance appear larger than traditional statistics. This lack of change in collagen organization is in agreement with no observed differences in collagen content.

Both the changes in elastin content and cathepsin expression are indicative of the dynamic nature of the ECM, which in turn leads to changes in the mechanical behavior. We know both the structure (number of lamella, thickness of fibers, degree of cross-linking, fiber orientation, etc.) and total quantity of components help determine the mechanical behavior of arteries and that these components constantly adapt to perturbations in an attempt to restore homeostatic levels of shear, circumferential, and axial stress (Wan et al., 2010); however, we also know that remodeling can also be maladaptive and result in progression towards disease. The administration of AZT in this study was shown to increase the stiffness of the arteries. This change could be due to a number of different parameters; the observed decreased elastin and increased thickening could contribute. The increase in intima-media thickness appeared to be due to thickening of the lamellar layers; however, we did not measure smooth muscle cell volume or number to determine if this contributed to the observed change.

Our study has several limitations. First, the mice were treated for 35 days, which is shorter than both the duration that humans receive antiretroviral drugs as well the development of atherosclerosis in humans; however, Shankar et al., 2005 showed endothelial dysfunction in only 4 weeks in healthy, HIV negative subjects who received the antiretroviral indinavir daily for that period, which suggest that HAART can induce changes in subjects within weeks. Another limitation is that the dosage of AZT administered was approximately 10 times higher than the human dose; note, however, that the half-life of AZT in the plasma of mice is around 5 times less than that of humans (Tan and Boudinot, 2000) and this dosage and time course was previously published; thus our methods are consistent with previous work (Sutliff et al., 2002; Lewis et al., 2000). Finally, while our mice did exhibit subclinical markers of atherosclerosis, they did not fully develop atherosclerosis. While we feel that the changes we observed were likely part of disease development rather than some sort of healthy, adaptive remodeling, the observance of the accelerated development of actual atherosclerotic lesions would be insightful.

In summary, the antiretroviral drug AZT has a number proatherogenic effects on the vasculature including arterial stiffening and carotid intima-media thickening. While a number of antiretroviral drugs including NRTIs have been implicated in leading to the development of atherosclerosis (Hsue et al., 2009; Lorenz et al., 2008), determining the specific role that the medications play in disease development is difficult since many patients have a number of confounding risk factors. This study used a mouse model to determine the isolated effects of AZT on otherwise healthy mice. We found that the mice exhibit the subclinical markers of atherosclerosis, which correlated to other changes that are not able to be determined clinically. These included changes in adventitial thickness, elastin quantity, and protease activity. This model serves as a good foundation for future studies to further investigate the AZT mitigated changes at a cellular level as well as to begin to investigate the changes due to the administration of one of the other drug classes.

Acknowledgments

We gratefully acknowledge the support from the American Heart Association (11GRNT7990055), National Institutes of Health and the International AIDS Society through the Creative and Novel Ideas in HIV Research (CNIHR) Program, and the National Science Foundation Graduate Research Fellowship Program (LH).

References

Bonnet D, Aggoun Y, Szezepanski I, Bellal N, Blanche S. Arterial stiffness and endothelial dysfunction in HIV-infected children. Aids. 2004; 18:1037–1041. [PubMed: 15096807]

Calmy A, Gayet-Ageron A, Montecucco F, Nguyen A, Mach F, Burger F, Ubolyam S, Carr A, Ruxungtham K, Hirschel B, Ananworanich J, Grp SS. HIV increases markers of cardiovascular risk: results from a randomized, treatment interruption trial. Aids. 2009; 23:929–939. [PubMed: 19425222]

Charakida M, Loukogeorgakis SP, Okorie MI, Masi S, Halcox JP, Deanfield JE, Klein NJ. Increased arterial stiffness in HIV-infected children: risk factors and antiretroviral therapy. Antiviral Therapy. 2009; 14:1075–1079. [PubMed: 20032537]

Chuong C, Fung Y. On residual stress in arteries. Journal of Biomechanical Engineering. 1986; 108:189–192. [PubMed: 3079517]

Dobrin P. Biaxial anisotropy of dog carotid artery: estimation of circumferential elastic modulus. Journal of Biomechanics. 1986; 19:351–358. [PubMed: 3733760]

El-Sadr WM, Lundgren JD, Neaton JD, Gordin F, Abrams D, Arduino RC, Babiker A, Burman W, Clumeck N, Cohen CJ, Cohn D, Cooper D, Darbyshire J, Emery S, Fatkenheuer G, Gazzard B, Grund B, Hoy J, Klingman K, Losso M, Mejia JMR, Markowitz N, Neuhaus J, Phillips A, Rappoport C. A. Strategies Management, 2006. CD4+count-guided interruption of antiretroviral treatment. New England Journal of Medicine. 2006; 355:2283–2296. [PubMed: 17135583]

Fernandez-Moure JS, Vykoukal D, Davies MG. Biology of aortic aneurysms and dissections. Methodist DeBakey Cardiovascular Journal. 2011; 7:2–7. [PubMed: 21979117]

Fisher SD, Miller TL, Lipshultz SE. Impact of HIV and highly active antiretroviral therapy on leukocyte adhesion molecules, arterial inflammation, dyslipidemia, and atherosclerosis. Atherosclerosis. 2006; 185:1–11. [PubMed: 16297390]

Friis-Møller N, Weber R, Reiss P, Thiébaut R, Kirk O, Monforte AdA, Pradier C, Morfeldt L, Mateu S, Law M, El-Sadr W, De Wit S, Sabin CA, Phillips AN, Lundgren JD. f. t. D. s. group, 2003. Cardiovascular disease risk factors in HIV patients-association with antiretroviral therapy. Results from the DAD study. Aids. 2003; 17:1179–1193. [PubMed: 12819520]

Gleason RL, Wilson E, Humphrey JD. Biaxial biomechanical adaptations of mouse carotid arteries cultured at altered axial extension. Journal of Biomechanics. 2007; 40:766–776. [PubMed: 16750537]

Hansen L, Parker I, Sutliff RL, Platt MO, Gleason RL Jr. Endothelial dysfunction, arterial stiffening, and intima-media thickening in large arteries from HIV-1 transgenic mice. Annals of Biomedical Engineering. 2012

Hebert V, Crenshaw B, Romanoff R, Ekshyyan V, Dugas T. Effects of HIV drug combinations on endothelin-1 and vascular cell proliferation. Cardiovascular Toxicology. 2004; 4:117–131. [PubMed: 15371629]

Holmberg SD, Moorman AC, Williamson JM, Tong TC, Ward DJ, Wood KC, Greenberg AE, Janssen RS. H. Investigators, 2002. Protease inhibitors and cardiovascular outcomes in patients with HIV-1. Lancet. 2002; 360:1747–1748. [PubMed: 12480430]

Hsue PY, Lo JC, Franklin A, Bolger AF, Martin JN, Deeks SG, Waters DD. Progression of atherosclerosis as assessed by carotid intima-media thickness in patients with HIV infection. Circulation. 2004; 109:1603–1608. [PubMed: 15023877]

Hsue PY, Hunt PW, Schnell A, Kalapus SC, Hoh R, Ganz P, Martin JN, Deeks SG. Role of viral replication, antiretroviral therapy, and immunodeficiency in HIV-associated atherosclerosis. AIDS. 2009; 23:1059–1067. [PubMed: 19390417]

Humphrey JD, Eberth JF, Dye WW, Gleason RL. Fundamental role of axial stress in compensatory adaptations by arteries. Journal of Biomechanics. 2009; 42:1–8. [PubMed: 19070860]

Jackson ZS, Gotlieb AI, Langille BL. Wall tissue remodeling regulates longitudinal tension in arteries. Circulation Research. 2002; 90:918–925. [PubMed: 11988494]

Kline ER, Sutliff RL. The roles of HIV-1 proteins and antiretroviral drug therapy in HIV-1-associated endothelial dysfunction. Journal of Investigative Medicine. 2008; 56:752–769. [PubMed: 18525451]

Lee HY, Oh BH. Aging and arterial stiffness. Circulation Journal: Official Journal of the Japanese Circulation Society. 2010; 74:2257–2262. [PubMed: 20962429]

Lewis W, Grupp IL, Grupp G, Hoit B, Morris R, Samarel AM, Bruggeman L, Klotman P. Cardiac dysfunction occurs in the HIV-1 transgenic mouse treated with zidovudine. Laboratory Investigation. 2000; 80:187–197. [PubMed: 10701688]

Li WA, Barry ZT, Cohen JD, Wilder CL, Deeds RJ, Keegan PM, Platt MO. Detection of femtomole quantities of mature cathepsin K with zymography. Analytical Biochemistry. 2010; 401:91–98. [PubMed: 20206119]

Liu J, Sukhova GK, Yang JT, Sun J, Ma L, Ren A, Xu WH, Fu H, Dolganov GM, Hu C, Libby P, Shi GP. Cathepsin L expression and regulation in human abdominal aortic aneurysm, atherosclerosis, and vascular cells. Atherosclerosis. 2005

Lorenz MW, Stephan C, Harmjanz A, Staszewski S, Buehler A, Bickel M, von Kegler S, Ruhkamp D, Steinmetz H, Sitzer M. Both long-term HIV infection and highly active antiretroviral therapy are independent risk factors for early carotid atherosclerosis. Atherosclerosis. 2008; 196:720–726. [PubMed: 17275008]

Lundgren JD, Neuhaus J, Babiker A, Cooper D, Duprez D, Ei-Sadr W, Emery S, Gordin F, Kowalska J, Phillips A, Prineas OJ, Reiss P, Sabin C, Tracy R, Weber R, Grund B, Neaton AD, Smart I, Grp DADS. Use of nucleoside reverse transcriptase inhibitors and risk of myocardial infarction in HIV-infected patients. Aids. 2008; 22:F17–F24. [PubMed: 18753925]

Maggi P, Lillo A, Perilli F, Maserati R, Chirianni A, Grp P. Colour-Doppler ultrasonography of carotid vessels in patients treated with antiretroviral therapy: a comparative study. Aids. 2004; 18:1023–1028. [PubMed: 15096805]

Mary-Krause M, Cotteb L, Simon A, Partisani M, Costagliola D, Clinical H. Epidemiology Grp French, 2003. Increased risk of myocardial infarction with duration of protease inhibitor therapy in HIV-infected men. Aids. 2003; 17:2479–2486. [PubMed: 14600519]

Ng CP, Hinz B, Swartz MA. Interstitial fluid flow induces myofibroblast differentiation and collagen alignment in vitro. Journal of Cell Science. 2005; 118:4731–4739. [PubMed: 16188933]

Oliviero U, Bonadies G, Apuzzi V, Foggia M, Bosso G, Nappa S, Valvano A, Leonardi E, Borgia G, Castello G, Napoli R, Sacca L. Human immunodeficiency virus per se exerts atherogenic effects. Atherosclerosis. 2009; 204:586–589. [PubMed: 19084229]

Platt M, Ankeny R, Shi G, Weiss D, Vega J, Taylor W, Jo H. Expression of cathepsin K is regulated by shear stress in cultured endothelial cells and is increased in endothelium in human

atherosclerosis. American Journal of Physiology: Heart and Circulatory Physiology. 2007; 292:H1479–H1486. [PubMed: 17098827]

Platt MO, Ankeny RF, Jo H. Laminar shear stress inhibits cathepsin L activity in endothelial cells. Arteriosclerosis Thrombosis Vascular Biology. 2006a; 26:1784–1790.

Platt MO, Xing Y, Jo H, Yoganathan AP. Cyclic pressure and shear stress regulate matrix metalloproteinases and cathepsin activity in porcine aortic valves. Journal of Heart Valve Disease. 2006b; 15:622–629. [PubMed: 17044366]

Ross AC, Storer N, O'Riordan M, Dogra V, El-Beijani D, Bhatt S, McComsey GA. Carotid intima-media thickness (cIMT) improves over time in HIV-infected children. Antiviral Therapy. 2008; 13:A18–A19.

Sevastianova K, Sutinen J, Westerbacka J, Ristola M, Yki-Jarvinen H. Arterial stiffness in HIV-infected patients receiving highly active antiretroviral therapy. Antiviral Therapy. 2005; 10:925–935. [PubMed: 16430198]

Shankar SS, Dube MP, Gorski JC, Klaunig JE, Steinberg HO. Indinavir impairs endothelial function in healthy HIV-negative men. American Heart Journal. 2005:150. [PubMed: 16084162]

Shi GP, Sukhova GK, Grubb A, Ducharme A, Rhode LH, Lee RT, Ridker PM, Libby P, Chapman HA. Cystatin C deficiency in human atherosclerosis and aortic aneurysms. Journal of Clinical Investigation. 1999; 104:1191–1197. [PubMed: 10545518]

Shi GP, Sukhova GK, Kuzuya M, Ye Q, Du J, Zhang Y, Pan JH, Lu ML, Cheng XW, Iguchi A, Perrey S, Lee AM, Chapman HA, Libby P. Deficiency of the cysteine protease cathepsin S impairs microvessel growth. Circulation Research. 2003; 92:493–500. [PubMed: 12600886]

Spieker LE, Karadag B, Binggeli C, Corti R. Rapid progression of atherosclerotic coronary artery disease in patients with human immunodeficiency virus infection. Heart and Vessels. 2005; 20:171–174. [PubMed: 16025368]

Sukhova GK, Shi GP, Simon DI, Chapman HA, Libby P. Expression of the elastolytic cathepsins S and K in human atheroma and regulation of their production in smooth muscle cells. Journal of Clinical Investigation. 1998; 102:576–583. [PubMed: 9691094]

Sukhova GK, Zhang Y, Pan JH, Wada Y, Yamamoto T, Naito M, Kodama T, Tsimikas S, Witztum JL, Lu ML, Sakara Y, Chin MT, Libby P, Shi GP. Deficiency of cathepsin S reduces atherosclerosis in LDL receptor-deficient mice. Journal of Clinical Investigation. 2003; 111:897–906. [PubMed: 12639996]

Sutliff R, Dikalov S, Weiss D, Parker J, Raidel S, Racine A, Russ R, Haase C, Taylor W, Lewis W. Nucleoside reverse transcriptase inhibitors impair endothelium-dependent relaxation by increasing superoxide. American Journal of Physiology: Heart and Circulatory Physiology. 2002; 283:H2363–H2370. [PubMed: 12388299]

Takamizawa K, Hayashi K. Strain energy density function and uniform strain hypothesis for arterial mechanics. Journal of Biomechanics. 1987; 20:7–17. [PubMed: 3558431]

Tan XL, Boudinot FD. Simultaneous determination of zidovudine and its monophosphate in mouse plasma and peripheral red blood cells by high-performance liquid chromatography. Journal of Chromatography B. 2000; 740:281–287.

Timmins LH, Wu QF, Yeh AT, Moore JE, Greenwald SE. Structural inhomogeneity and fiber orientation in the inner arterial media. American Journal of Physiology-Heart and Circulatory Physiology. 2010; 298:H1537–H1545. [PubMed: 20173046]

van Vonderen MGA, Smulders YM, Stehouwer CDA, Danner SA, Gundy CM, Vos F, Reiss P, van Agtmael MA. Carotid intima-media thickness and arterial stiffness in HIV-infected patients: the role of HIV, antiretroviral therapy, and lipodystrophy. Jaids-Journal of Acquired Immune Deficiency Syndromes. 2009; 50:153–161.

van Vonderen MGA, Hassink EAM, van Agtmael MA, Stehouwer CDA, Danner SA, Reiss P, Smulders Y. Increase in carotid artery intima-media thickness and arterial stiffness but improvement in several markers of endothelial function after initiation of antiretroviral therapy. Journal of Infectious Diseases. 2009; 199:1186–1194. [PubMed: 19275490]

Wagenseil JE, Nerurkar NL, Knutsen RH, Okamoto RJ, Li DY, Mecham RP. Effects of elastin haploinsufficiency on the mechanical behavior of mouse arteries. American Journal of Physiology. Heart and Circulatory Physiology. 2005; 289:H1209–H1217. [PubMed: 15863465]

Wan W, Gleason RL. Biomechanical and microstructural properties of common carotid arteries from fibulin-5 null mice. Annals of Biomedical Engineering. 2010; 38:3605–3617. [PubMed: 20614245]

Wan W, Gleason RL Jr. Dysfunction in elastic fiber formation in fibulin-5 null mice abrogates the evolution in mechanical response of carotid arteries during maturation. American Journal of Physiology. Heart and Circulatory Physiology. 2012

Wan W, Yanagisawa H, Gleason R. Biomechanical and microstructural properties of common carotid arteries from fibulin-5 null mice. Annals of Biomedical Engineering. 2010; 38:3605–3617. [PubMed: 20614245]

Wan W, Hansen L, Gleason RL. A 3-D constrained mixture model for mechanically mediated vascular growth and remodeling. Biomechanics and Modeling in Mechanobiology. 2010; 9:403–419. [PubMed: 20039091]

Wan W, Dixon JB, Gleason Rudolph L. Constitutive modeling of mouse carotid arteries using experimentally measured microstructural parameters. Biophysical Journal. 2012; 102:2916–2925. [PubMed: 22735542]

Wang XW, Chai H, Yao QZ, Chen CY. Molecular mechanisms of HIV protease inhibitor-induced endothelial dysfunction. Jaids-Journal of Acquired Immune Deficiency Syndromes. 2007; 44:493–499.

Wilder CL, Park KY, Keegan PM, Platt MO. Manipulating substrate and pH in zymography protocols selectively distinguishes cathepsins K, L, S, and V activity in cells and tissues. Archives of Biochemistry and Biophysics. 2011; 516:52–57. [PubMed: 21982919]

Worm SW, Sabin C, Weber R, Reiss P, El-Sadr W, Dabis F, De Wit S, Law M, Monforte AD, Friis-Moller N, Kirk O, Fontas E, Weller I, Phillips A, Lundgren J, Grp DADS. Risk of myocardial infarction in patients with HIV infection exposed to specific individual antiretroviral drugs from the 3 major drug classes: The data collection on adverse events of anti-HIV drugs (D:A:D) study. Journal of Infectious Diseases. 2010; 201:318–330. [PubMed: 20039804]

Zoumi A, Lu XA, Kassab GS, Tromberg BJ. Imaging coronary artery microstructure using second-harmonic and two-photon fluorescence microscopy. Biophysical Journal. 2004; 87:2778–2786. [PubMed: 15454469]

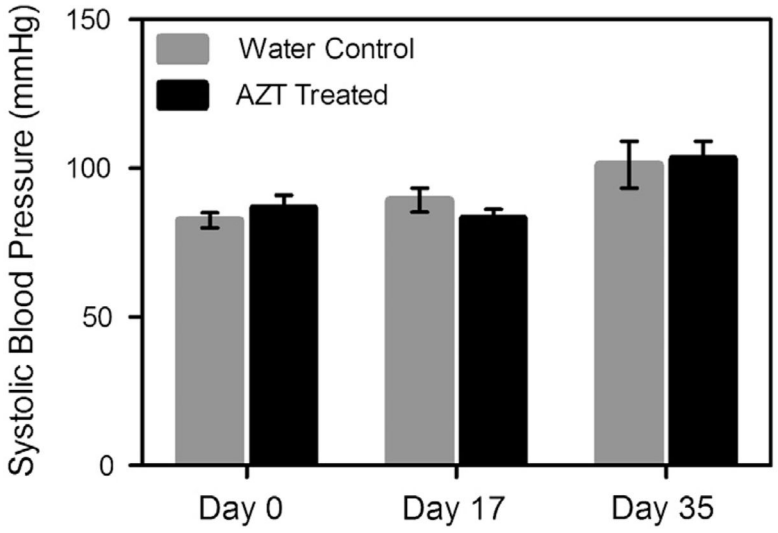

Fig. 1.

Blood pressure does not differ between groups. The blood pressure of the mice was determined using a tail-cuff blood pressure system. Pressures were measured at days 0 17, and 25 of treatment initiation. No differences were noted between groups at any time point (n = 7).

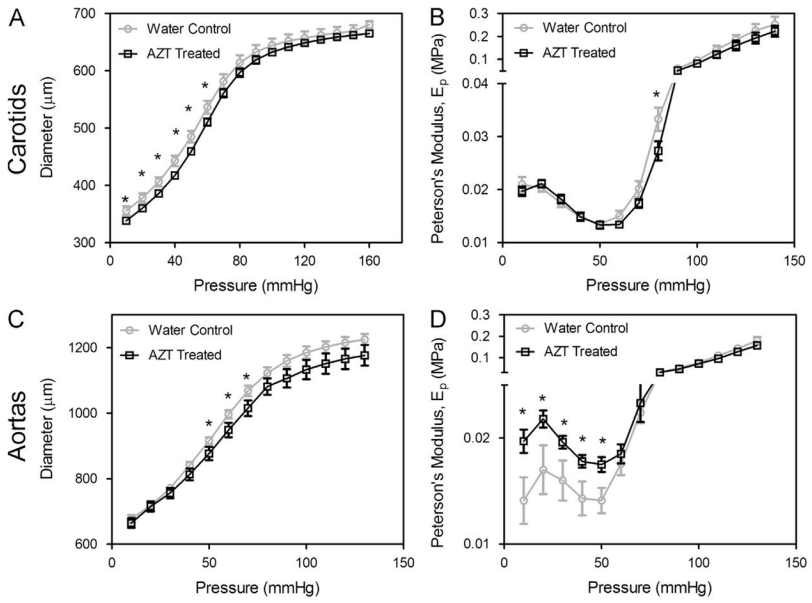

Fig. 2.

AZT treatment increases arterial stiffness. Mechanical testing was used to investigate the biomechanics of carotid arteries (A and B) and aortas (C and D). Pressure–diameter mechanical tests (A & C) were performed at a series of fixed stretches. Peterson's modulus, E_p, of the vessels was used to normalize for differences in vessel geometry (B & D, * indicates $p < 0.05$, $n = 6$ (carotids), $n = 9$ (aortas), and data is mean ± SEM).

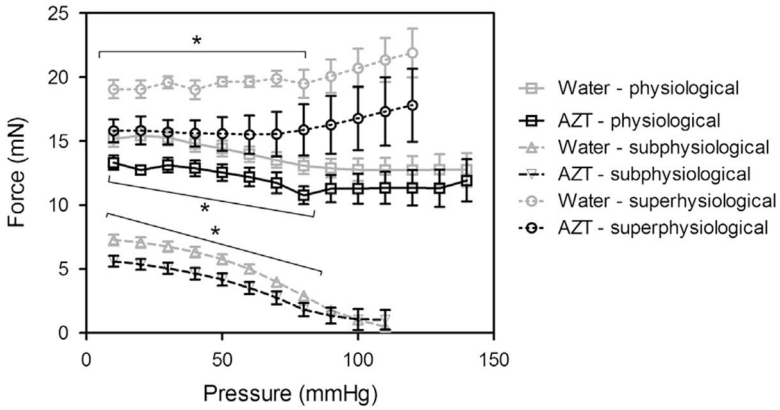

Fig. 3.

AZT treatment decreases axial force during pressure–diameter tests. Axial force was also measured during the pressure–diameter mechanical tests. Analysis of the axial force revealed that the AZT treated mice had significantly lower forces at pressures from 10–80 mmHg for the subphysiological and physiological stretch and from 10–70 mmHg for the superphysiological stretch. (■ is physiological stretch, ▲ is subphysiological stretch, and ● is superphysiological stretch, * indicates $p < 0.05$, $n = 8$, and data is mean ± SEM). No differences were found in the carotids.

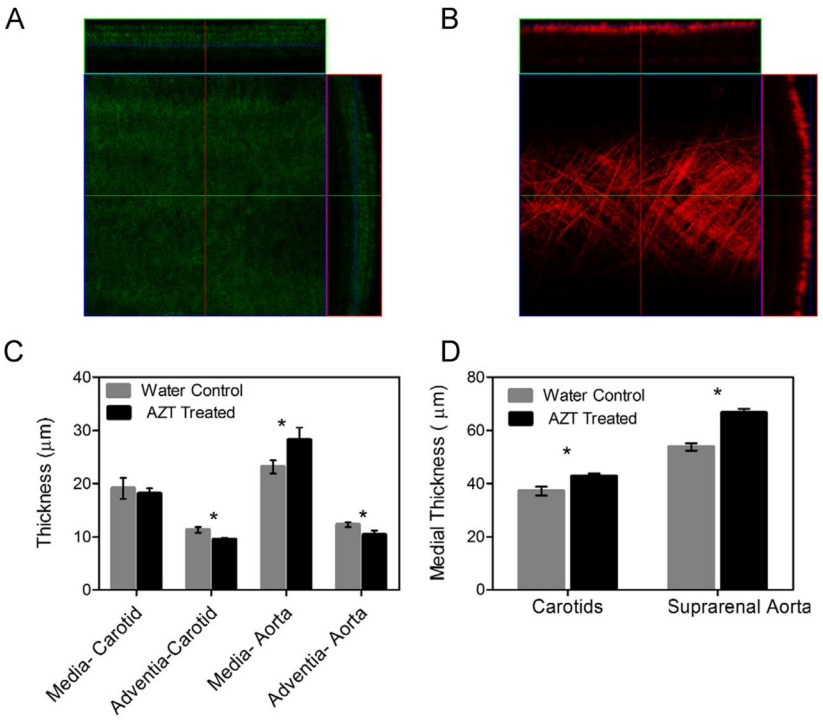

Fig. 4.

AZT treatment increases intima-media thickness. Thickness of the arteries was calculated using cross-sectional views from multiphoton microscopy stacks of arteries under a physiological load and histology cross-sections. Panel A shows a representative elastin slice and cross-section from an AZT treated aorta and panel B shows a collagen slice and cross section from the same vessel. The calculated intima-media thickness in the AZT treated mice increased in the aorta, while the adventitia was decreased in both the aortas and carotids (C). The intima-media thickness calculated from fixed/frozen histological slides stained with H&E also showed intima-media thickening for both carotids and aortas (D). (* indicates $p < 0.05$, $n = 6$, data is mean ± SEM).

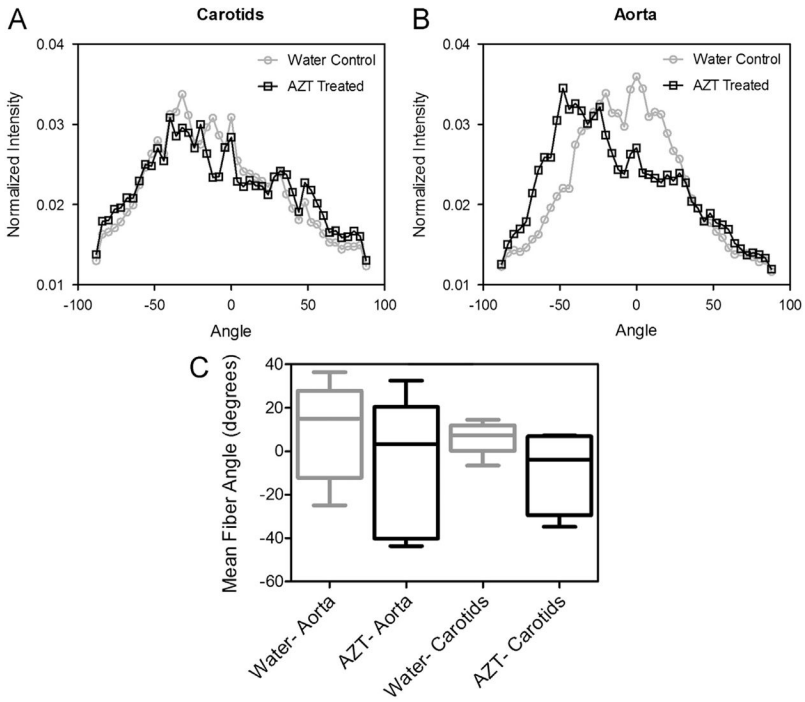

Fig. 5.

AZT treatment does not affect collagen fiber angles. The distribution of collagen fibers within the adventitia was determined using fast Fourier transform techniques on images from the multiphoton microscopy z-stacks. Histograms of the mean normalized intensities are shown in A for the carotids and B for the aortas. Panel C shows a box and whisker plot of the weighted mean angle from each vessel was calculated using circular statistical methods and no differences were found between the weighted circular means of the groups (C). (n = 6, data is circular mean and 0–95 percentiles, $p < 0.05$).

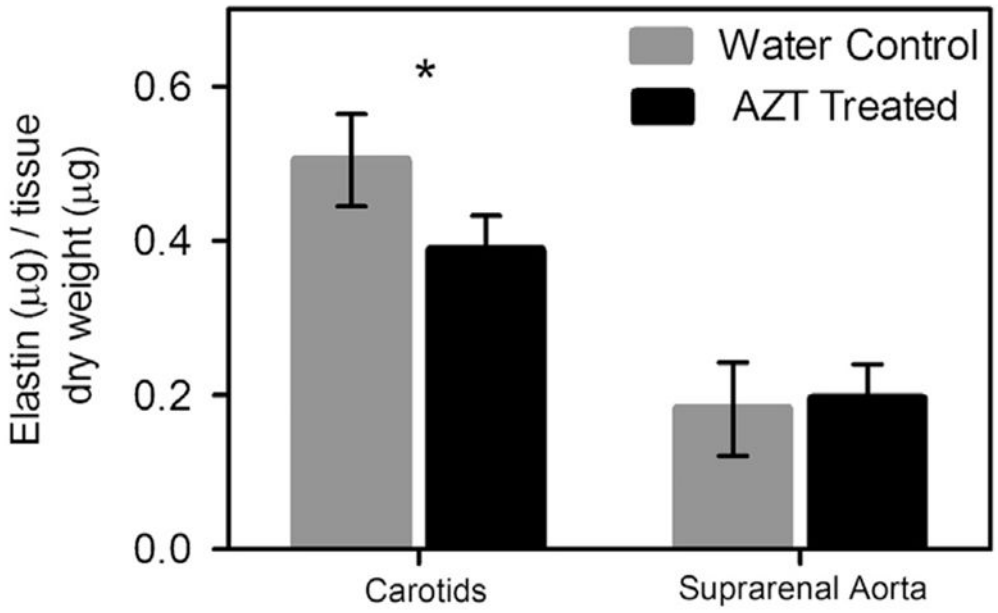

Fig. 6.

AZT treatment decreases elastin content. Elastin and collagen content of the arteries was assessed using the Fastin and Sirius red assays. The carotids from AZT treated mice had less elastin than the water control mice. (* indicates $p < 0.05$, $n = 6$, and data is mean ± SEM). No difference in the collagen content of the arteries was observed. (not shown, $n = 6$).

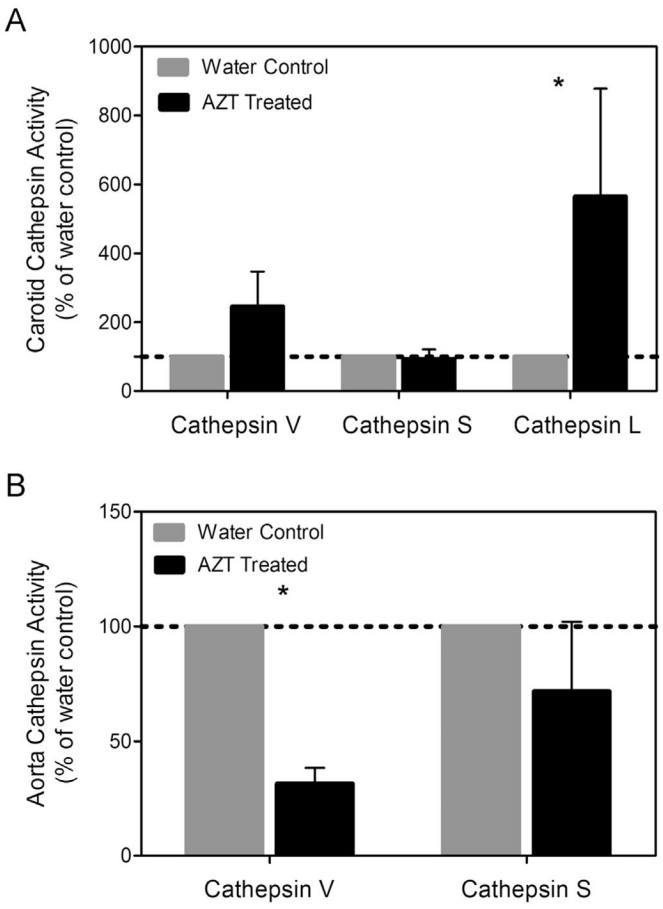

Fig. 7.

AZT alters cathepsin L activity. The level of activity of cathepsins S and L was assessed using zymography. (A) Densitometric analysis of the carotids revealed an increase in cathepsin L, while analysis of the aortas showed decreases in cathepsin L activity. (B) (n = 4, $p < 0.05$, and data is mean ± SEM).